The Importance of Biological Particles to the Ice Nucleating Particle Concentration in a Coastal Tropical Site

Luis A. Ladino[1,*], Graciela B. Raga[1], Harry Alvarez-Ospína[2], Manuel A. Andino-Enríquez[3], Irma Rosas[1], Leticia Martínez[1], Eva Salinas[1], Javier Miranda[4], Zyanya Ramírez-Díaz[1], Bernardo Figueroa[5], Cedric Chou[6], Allan K. Bertram[6], Erika T. Quintana[7], Luis A. Maldonado[8], Agustín García-Reynoso[1], Meng Si[6], and Victoria E. Irish[6]

[1]Centro de Ciencias de la Atmosfera, Universidad Nacional Autonoma de Mexico, Mexico City, Mexico
[2]Facultad de Ciencias, Universidad Nacional Autonoma de Mexico, Mexico City, Mexico
[3]School of Chemical Sciences and Engineering, Universidad Yachay Tech, Ecuador
[4]Instituto de Fisica, Universidad Nacional Autonoma de Mexico, Mexico City, Mexico
[5]Laboratorio de Ingenieria y Procesos Costeros, Instituto de Ingenieria, Universidad Nacional Autonoma de Mexico, Sisal, Yucatan, Mexico
[6]Chemistry Department, University of British Columbia, Vancouver, Canada.
[7]Escuela Nacional de Ciencias Biologicas, Instituto Politecnico Nacional, Mexico City, Mexico
[8]Facultad de Quimica, Universidad Nacional Autonoma de Mexico, Mexico City, Mexico

Correspondence to: Luis A. Ladino (luis.ladino@atmosfera.unam.mx)

Abstract. Atmospheric aerosol particles that can nucleate ice are referred to as ice nucleating particles (INP). Recent studies have confirmed that aerosol particles emitted by mid- and high-latitude oceans can act as INPs. This very relevant information can be included in climate and weather models to predict the formation of ice in clouds, given that most of them do not consider the oceans as

5 a source of INPs. Very few studies to sample INPs have been carried out in tropical latitudes, and there is a need to evaluate their availability to understand the potential role that marine aerosol may play in the hydrological cycle of tropical regions.

This study presents results from the first measurements obtained during a field campaign con-

10 ducted in the topical village of Sisal, located on the coast of the Gulf of Mexico of the Yucatan peninsula in Mexico in January-February 2017, and one of the few data sets currently available at similar latitudes. Aerosol particles sampled in Sisal are shown to be very efficient INPs, with onset freezing temperatures as high as -3 °C (in some cases), similar to the onset temperature for *Pseudomonas syringae*. The results show that the INP concentration in Sisal is higher than at other

15 locations sampled with the same type of INP counter. Air masses arriving in Sisal during the passage of cold fronts have, surprisingly, higher INP concentrations than the campaign-average, despite their lower total aerosol concentration.

Biological particles were likely found to be very important in ice cloud formation at this tropical

location, given the large concentration of INPs above -12°C. A variety of bacteria and fungi were
20   identified. Although the majority are of terrestrial origin, some of them are clearly oceanic.

1   Introduction

Clouds are essential to the hydrological cycle of the planet and also play a significant role in the
radiative balance of the climate system (Ramanathan et al., 1989; Lohmann and Feichter, 2005;
Andreae and Rosenfeld, 2008; Stevens and Feingold, 2009). Cloud formation depends on the pres-
25   ence of cloud condensation nuclei (CCN) and most precipitation from mixed-phase clouds involves
also the presence of ice nucleating particles (INPs). Aerosol-cloud interactions are one of the main
sources of uncertainty in climate projections as assessed by the Intergovernmental Panel on Climate
Change (Stocker et al., 2013), prompting large research efforts from the scientific community in
recent years. Nevertheless, the formation and evolution of ice crystals in mixed-phase and cirrus
30   clouds still remain highly uncertain (Seinfeld et al., 2016; Kanji et al., 2017; Field et al., 2017).
Several pathways have been proposed as potentially responsible for ice formation: condensation
freezing, contact freezing, immersion freezing, and deposition nucleation (Vali et al., 2015). Murray
et al. (2012) and Ladino et al. (2013) have suggested that contact freezing and immersion freezing
are the most efficient mechanisms leading to ice nucleation in clouds; however, the atmospheric
35   relevance of contact freezing is still under debate (Murray et al., 2012; Kanji et al., 2017).

Most of the precipitation from deep convection in the tropics, e.g. in the Inter-tropical Conver-
gence Zone, forms via the ice phase (Mülmenstädt et al., 2015). Given the potential INP role of a
variety of aerosol particles such as mineral dust, biological particles, crystalline salts, carbonaceous
particles, and secondary organic aerosol, the main source of INPs at tropical latitudes is highly un-
40   certain (Kanji et al., 2017; Yakobi-Hancock et al., 2014; DeMott et al., 2010). Although it is yet
not fully understood what exactly makes an aerosol particle an efficient INP, its composition, active
sites, crystal structure, size, or hygroscopicity, there is evidence that their composition is one of the
key factors (Kanji et al., 2017). Mineral dust has been recognized as the most important INP on a
global scale due to their good ice nucleating abilities and their elevated concentrations in the tro-
45   posphere (Hoose and Möhler, 2012; Nenes et al., 2014; Atkinson et al., 2013; Kanji et al., 2017).
Bioaerosol has also been identified as very efficient INP (Kanji et al., 2017; Hoose and Möhler,
2012; Fröhlich-Nowoisky et al., 2016; Hill et al., 2017) with onset freezing temperatures as high as
-2 °C (Yankofsky et al., 1981; Després et al., 2012; Fröhlich-Nowoisky et al., 2015; Wex et al., 2015;
Stopelli et al., 2017). Global climate models parameterize cloud droplet and ice crystal formation
50   from observational studies and results from such modelling suggest that on a global scale bioaerosol
are not a major INP source and therefore have a lower impact in ice cloud formation, in comparison
to mineral dust particles (Hoose et al., 2010; Sesartic et al., 2012); however, this may not be the case
on a regional scale (Burrows et al., 2013; Mason et al., 2015a). Such models also suggest that the

most important oceanic sources of INPs are the southern oceans, north Atlantic, and north Pacific
55 (Burrows et al., 2013; Yun and Penner, 2013; Wilson et al., 2015; Vergara-Temprado et al., 2017);
however, those conclusions were drawn with little or no data from tropical latitudes.

Although important efforts were made during the 1950-70's to understand the role of the oceans
in ice cloud formation (Schnell and Vali, 1975; Schnell, 1975, 1977, 1982; Rosinski et al., 1987,
1988), recently new and robust evidence that biological material from marine environments could
60 act as efficient INPs have been reported (Knopf et al., 2011; Wilson et al., 2015; Mason et al., 2015b;
DeMott et al., 2016; Ladino et al., 2016; McCluskey et al., 2017; Irish et al., 2017; Welti et al., 2018).
Most of the past available INP data were obtained from mid- and high-latitudes studies, with tropical
latitudes heavily under represented (Schnell, 1982; Rosinski et al., 1987, 1988; Boose et al., 2016;
Welti et al., 2018; Price et al., 2018). Marine and coastal INP concentration ([INP]) typically ranges
65 from 10^{-4} L^{-1} to 10^{-1} L^{-1} for temperatures between -10 °C and -25 °C (Kanji et al., 2017), but
have shown to be higher at tropical coastal sites (Rosinski et al., 1988; Boose et al., 2016; Welti
et al., 2018; Price et al., 2018). This large [INP] range may strongly depend on the microbiota
concentration, the marine biological activity, and the organic matter enrichment in the sea surface
microlayer as shown in Wilson et al. (2015).

70 At marine and coastal sites, a large variety of bacteria have been identified with *Proteobacteria*,
Firmicutes, and *Bacteroidetes* as the main reported phyla (Després et al., 2012). Also, airborne
fungi are common in both continental and marine environments with *Cladosporium*, *Alternaria*,
Penicillium, *Aspergillus*, and *Epicoccum* the main identified genus (Després et al., 2012). Besides
bacteria and fungal spores, viruses, algae, and pollen have also been identified in the bioaerosol of
75 marine environments (Després et al., 2012; Fröhlich-Nowoisky et al., 2015; Michaud et al., 2018).
Therefore, the concentration, ice nucleating abilities, and variability of tropical bioaerosol need to
be better characterized to quantify their role in cloud formation and precipitation development at
regional level and within the tropical zonal band.

The Yucatan peninsula, surrounded by the Gulf of Mexico to the West and the Caribbean sea to the
80 East, with a large variety of tropical vegetation, is a great source of both terrestrial and marine mi-
croorganisms (Guzmán, 1982; Videla et al., 2000; Morales et al., 2006). Tropical cyclones (TC) and
cold fronts are some of the meteorological phenomena that seasonally affect the Yucatan peninsula
every year (Whigham et al., 1991; Landsea, 2007; Knutson et al., 2010). DeLeon-Rodriguez et al.
(2013) show that TC can significantly enhance the concentration of biological particles throughout
85 the troposphere and can also efficiently transport biological particles far away from their sources.
Moreover, Mayol et al. (2017) showed that ocean and terrestrial microorganisms can be efficiently
transported long distances from their sources over the tropical and subtropical oceans.

This study present results of the concentration of INPs as a function of temperature and particle
size, and the concentration and composition of biological particles at a tropical coastal site (Sisal,
90 Yucatan) with the goal to infer the importance of biological particles in mixed-phase cloud formation

and precipitation development.

2 Methods

2.1 Sampling site

Ambient aerosol particles were collected and characterized between January 21 and February 02,
2017 in the coastal village of Sisal, located in the northwest corner of the Yucatan peninsula (21°0955N
90°0150W), as shown in Figure 1. Sisal had 1837 inhabitants in 2015 (SEDESOL, 2015), with fish-
ing and tourism being the main economical activities. The closest industry is located approximately
25 km away from the village and the nearest city is Merida, 75 km away.

The instruments used in this study were located on the roof of the Engineering Institute building
of the Universidad Nacional Autonoma de Mexico (UNAM, Sisal Campus) which is 50 m from the
shoreline and about 1.7 km from the center of Sisal (Figure 1). The roof is 25 m above ground level
and directly faces the ocean.

January and February are part of the cold dry season in Mexico, with isolated events of rain
associated with cold fronts reaching the deep tropics. The average temperature and relative humidity
(RH) during the sampling period were 22.3 ± 3.6 °C and 68.9 ± 6.2 %, respectively.

2.2 Instrumentation

A suite of instrumentation was deployed in Sisal to characterize the aerosol chemical composition,
concentration, size distribution, biological content, INPs concentration, and meteorological variables
(Table 1). Most instruments were run simultaneously and next to each other (less than 10 m apart)
and only wet aerosol particles were sampled. Additionally, none of the instrumentation used an
impactor or cyclone prior to their inlets. The inlets were located around 1.5 m - 2.0 m above the roof
surface. The meteorological data was obtained with a meteorological station (Davis, VANTAGE
PRO2) placed in a different building approximately 20 m away for the other instruments.

2.2.1 Aerosol concentration and size distribution

The aerosol particle concentration and size distribution was monitored with a condensation particle
counter (CPC 3010, TSI) and with an optical particle counter (LasAir II 310A, PMS), respectively.
The total particle concentration reported by the CPC was collected every second at a flow rate of
1 L min^{-1}, whereas the aerosol concentration as function of size (cut-sizes at 0.3 μm, 0.5 μm,
1.0 μm, 5.0 μm, 10.0 μm, and 25 μm) was recorded every 11 s with the LasAir at a flow rate
28.3 L min^{-1}.

2.2.2 Ice nucleating particles

To determine the INP concentrations in the ambient air, aerosol particles were collected on hydrophobic glass cover slips (HR3-215; Hampton Research) with the help of a Micro-Orifice Uniform Deposit Impactor (MOUDI 110R, MSP). Identical substrate holders as those described in Mason et al. (2015a) were used to keep the glass coverslips at a location on the impaction plate where particle concentrations varied by a relatively small amount. The MOUDI has eight stages at which particles are separated and collected as a function of their aerodynamic diameter (cut-sizes are 0.18 μm, 0.32 μm, 0.56 μm, 1.0 μm, 1.8 μm, 3.2 μm, 5.6 μm, and 10.0 μm). The flow through the MOUDI is 30 L min^{-1} and the typical sampling time was 6 h. It has been recognized that when sampling with a MOUDI under dry conditions (i.e, RH below approximately 60 %), aerosol particles can bounce from the impaction plates moving to lower stages (Winkler, 1974; Chen et al., 2011; Bateman et al., 2014). Although this is a known artifact when using this technique, this may not have been an issue in the current study given that the ambient RH was typically above 67 %. The glass substrates containing the ambient aerosol particles were stored in petri dishes at 4 °C prior to their analysis.

The INP concentrations were measured with a cold cell coupled to an optical microscope with an EC Plan-Neofluar 5 X objective (Axiolab, Zeiss) following the MOUDI-DFT method described by Mason et al. (2015a). Activation scans were conducted between 0 °C and -40 °C at a cooling rate of -10 °C per minute for particles collected on stages two to seven. Stage one was not taken into account given that the aerosol concentration on the glass substrates was typically very low, whereas in stage eight the number concentration of particles deposited on the glass substrates was too high which inhibited the proper formation of water drops.

2.2.3 Chemical composition

A second MOUDI (100NR, MSP) was operated simultaneously to collect aerosol particles for chemical composition analysis with particle sizes ranging from 0.18 μm to 10.0 μm. Particles were collected on 47 mm Teflon filters (Pall Science) for 48 h at a flow rate of 30 L min^{-1}. The filters were weighed prior and after the sampling and stored in petri dishes at 4 °C until they were analyzed. The filters were first analyzed for elemental composition and followed by ion-cation concentration analysis, performing two different analyses on each filter.

Elemental composition of the aerosol samples was determined by X-ray fluorescence (XRF), using the x-ray spectrometer at Laboratorio de Aerosoles, Instituto de Fisica, UNAM (Espinosa et al., 2012). The samples were mounted on plastic frames with no previous treatment. The analysis was carried out using an Oxford Instrument (Scotts Valley, CA, USA) x-ray tube with an Rh anode and an Amptek (Bedford, MA, USA) Silicon Drift Detector (resolution 140 eV at 5.9 keV). The tube operated at 50 kV and a current of 500 μA, irradiating during 900 s per spectrum. The efficiency of

the detection system was measured using a set of thin film standards (MicroMatter Co., Vancouver, Canada). The spectra obtained for the samples were deconvolved with the WinQXAS computer code (IAEA, 1997), and the experimental uncertainties in elemental concentrations were computed according to the method described by Espinosa et al. (2010).

160   After the XRF analysis, the Teflon filters were analyzed for NO_3^-, SO_4^{2-}, Cl^-, K^+, Na^+, Ca^{2+}, Mg^{2+}, and NH_4^+ using a Dionex model ICS-1500, equipped with an electrical conductivity detector, with following Chow and Watson (1999). NO_3^-, Cl^-, and SO_4^{2-} were separated using a Thermo Scientific Dionex IonPac AS23-4 μm Analytical Column (4 mm x 250 mm) with Thermo Scientific Dionex CES 300 Capillary Electrolytic Suppressor module. The injection volume was 1000 μL, mo-

165 bile phase was 4.5 mM Na_2C0_3 - 0.8 mM NaHCO at 1 mL min^{-1} flow rate. For NH_4^+, Na^+, Ca^{2+}, Mg^{2+}, and K^+, volumes of 1000 μL were injected in a Thermo Scientific Dionex IonPac CS12A Cation-Exchange Column (4 mm x 250 mm) with the Thermo Scientific Dionex CES 300 Capillary Electrolytic Suppressor. The mobile phase was a solution CH_4SO_3 20 mM and 1 mL min^{-1} flow rate.

170   2.2.4   Biological particles

Air samples were collected using two Quick Take 30 Sample Pump BioStage viable cascade impactor (SKC Inc. USA), which is a one-stage portable battery-powered instrument operated at a constant airflow rate (28.3 L min^{-1}) for a sampling time of 5 min. Petri dishes containing Trypticase soy agar (TSA; BD Bioxon) media, supplemented with 100 mg L^{-1} cycloheximide (Sigma-

175 Aldrich) to prevent fungal growth, were used for capture cultivable total bacteria, and Malt extract agar (EMA; BD Bioxon) for cultivable airborne propagule fungi. The two impactors, one with the TSA and the other one with EMA growing media, were run in parallel. After exposure, the plates were incubated at 37 °C during 24 h - 48 h for cultivable total bacteria and at 25 °C during 48 h - 72 h for propagule fungi. After incubation, colonies growing on each plate were counted and concentra-

180 tions were calculated by taking the sampling rates into account and reported as colony-forming units per cubic meter (cfu m^{-3}) of air. The petri dishes with the grown colonies were stored at 4 °C prior to their analysis. Fungi were identified to genus level by macroscopic characteristics of the colonies and microscopic examination of the spore structure. Representative bacterial colonies were picked and purified using several transfer steps of single colonies on TSA and checked by Gram-staining

185 and microscopy. Fresh biomass of the bacterial isolates were suspended in 30 % glycerol LB-broth (Alpha Biosciences, Inc.) and stored at -72 °C, for further analyses.

     Bacteria isolated from the pure cultures were identified by 16S rRNA sequencing. DNA was extracted using the QIAamp DNA Mini kit (QIAGEN), according to the manufacturers protocol. Partial 16S rRNA gene sequences were amplified by polymerase chain reaction (PCR) using univer-

190 sal bacterial primers 27F (5-AGA GTT TGA TCM TGG CTC AG-3) and 1492R (5-TAC GGY TAC CTT GTT ACG ACT T-3) (Lane, 1991). PCRs were performed in a total volume of 50 μL including

2 μL of bacterial DNA, 35.4 μL of ddH$_2$O, 5 μL of 10 X buffer, 1.5 μL of MgCl$_2$ (1.5 mM), 1 μL of dNTPs (10 mM), 0.1 μL of Taq DNA polymerase (5 U μL^{-1}), and 2.5 μL each primer (10 μM). Cycle conditions were as follows: initial denaturation at 94 °C for 1 min; followed by 35 cycles at 94 °C for 1 min, 56 °C for 30 s, 72 °C for 1.5 min; and a final extension at 72 °C for 5 min. The PCR products were examined for size and yield using 1.0 % (w/v) agarose gels in TAE buffer. After successful amplification, the obtained products were sequenced using a PRISM 3730 automated sequencer (Applied Biosystem Inc.). DNA sequences were edited and assembled using the Seq-Man and Edit Seq software (Chromas Lite, Technely Slom Pty Ltd. USA). Sequence similarity analysis was performed using the BLAST software (http://www.ncbi.nlm.nih.gov/BLAST).

Although specific growing media for actinobacteria were not used in this study, some actinobacteria colonies were able to grow on the TSA petri dishes; therefore, in some cases they were isolated and identified as follows. Genomic DNA was extracted using standard protocols reported previously for actinobacteria (Maldonado et al., 2009). The DNA preparations were then used as template for 16S rRNA gene amplification using the universal set of bacterial primers 27f and 1525r (Lane, 1991). The following components for the PCR mix were employed: 0.5 μL DNA template (for a final concentration of 100 ng μL^{-1}, 5 μL 10X DNA polymerase buffer, 1.5 μL MgCl$_2$ (50 mM stock solution), 1.25 μL dNTP (10 mM stock mixture), 0.5 μL of each primer (20 μM stock solution), 2.0 units of Taq polymerase made up to 50 μL with deionized sterile distilled water.

The PCR amplification was achieved using a Techne 512 gradient machine using the protocol described in Maldonado et al. (2008). The expected product (size aprox 1,500 bp) was checked by horizontal electrophoresis (70 V, 40 min) and then purified using the QIAquick PCR purification kit (QIAGEN, Germay) following the manufacturers instructions. Purified 16S rRNA gene PCR products were sent for sequencing to Macrogen (Korea) for the DyeDeoxy Terminator Cycle Sequencing kit (Applied Byosystems). Assembly of each 16S rRNA gene sequence was performed using Chromas (www.technelysium.com.au) and checked manually with the SeaView software (Galtier et al., 1996). Each assembled sequence was compared against two databases, namely, (a) the GenBank database (www.ncbi.nlm.nih.gov) by using the BLAST option and (b) the EZCloud (www.ezbiocloud.net) under its EZTaxon option. Both databases generated a list of the closest phylogenetic neighbors to each sequence and the EZTaxon, specifically provided the list of the closest described (type) species. At least 650 bp were employed for the analyzes.

3 Results and Discussion

3.1 Aerosol Concentration and Meteorology

Figure 2 shows the time series of the aerosol particle concentration between January 21 and February 02, 2017. Note the large diurnal variability for the aerosol particle concentration measured by the CPC (particles > 30 nm) and the LasAir (particles >300 nm), with average concentrations for the

entire sampling period of 896±570 cm^{-3} and 0.026±0.022 cm^{-3}, respectively. The data reported by the CPC and the LasAir indicate that most of the aerosol particles were smaller than 300 nm. A similar result was found by Rosinski et al. (1988) in the Gulf of Mexico (GoM) who found that

230   the aerosol concentration for particles ranging between 0.5 μm and 1.0 μm was three to four orders of magnitude smaller than particles ranging between 0.003 μm and 0.1 μm. A decrease in aerosol particle concentration was observed at the arrival and during the passage of two cold fronts (indicated by the vertical grey areas in Fig. 2 and labeled A and B) during the sampling period. Associated with the arrival of the cold fronts, horizontal wind speed at the site increased by at least a factor of three,

235   as seen in Figure 3. During cold front A, the wind direction was almost constant from approximately 270 °, while during the cold front B the wind direction varied between 270 ° and 360 °, with a more northerly component and a larger influence from the GoM compared to winds associated with cold front A.

Hysplit back-trajectories from the measurement site were run for 72 h for each of the days of the

240   campaign. In the absence of cold fronts A and B, the air masses arriving in Sisal had a very likely large continental influence, associated with southerly winds (Figure S1). However, when the cold fronts A and B reached the Yucatan Peninsula, northerly and northwesterly winds prevail, associated with more marine influence. The arrival of the cold fronts was also confirmed with the National Oceanic and Atmospheric Administration (NOAA) surface maps for January 22 and 29 (Figure S2).

245   Air masses behind both cold fronts, flowing over the GoM, were characterized by lower aerosol particle concentrations than air masses coming from the south to the site. This result agrees well with a large body of evidence indicating that marine air masses have lower aerosol particle concentration than continentally-influenced air masses (Patterson et al., 1980; Fitzgerald, 1991). Note, however that the number size distributions of the aerosol particles larger than 300 nm did not significantly

250   change before, during or after the passage of the cold fronts (Figure S3).

3.2   Ice Nucleating Particle Concentration ([INP])

A total of 41 samples (8 stages each) were collected during the Sisal field campaign to calculate the [INP] as a function of temperature and particle size. Some of these samples showed a high ice nucleating activity with high [INP] at temperatures close to 0 °C. In some cases the onset freezing

255   temperatures were found to occur at temperatures as high as -3 °C. Figure 4 summarizes the [INP] as a function of temperature for 29 analyzed samples (bluish area with red edges). Due to technical issues it was not possible to analyze the samples collected after January 30th. The present results are superimposed on the data reported by Kanji et al. (2017) to conduct a direct comparison with previous studies.

260   At temperature above -12 °C the [INP] measured in Sisal was slightly higher than the values reported by DeMott et al. (2016) at the continental boundary layer in the US. Aerosol particles acting as INPs at these warm temperatures are usually recognized as biological given that other

aerosol particles such as metals, crystalline salts, combustion particles (e.g., soot), and organics are unable to nucleate ice crystals under these conditions. Moreover, for typical concentrations of

265 mineral dust in the atmosphere, ice nucleation by mineral dust at these temperatures is not important (Hoose and Möhler, 2012; Murray et al., 2012; Kanji et al., 2017). The potential sources of the measured INPs in Sisal are discussed below.

Figure 5 is based on Mason et al. (2016) and shows the average [INP] for three different temperatures (-15 °C, -20 °C, and -25 °C) at different locations around the globe using the same sampling

270 and analysis methods. The Sisal data corresponds to particle diameters ranging between 0.32 μm and 10 μm where 16 out of the 29 samples fulfilled the size criteria. At -15 °C the average [INP] in Sisal was lower than Kolby (USA) and Labrador Sea; however, the obtained values are comparable to those found at UBC (Canada), Saclary (France), and Ucluelet (Canada). At -20 °C and -25 °C the average [INP] in Sisal were comparable or higher than at the other locations. As shown by the stars

275 on top of the Sisal bars, the [INP] during the passage of the cold fronts was found to be higher than the average [INP] although the obtained values are within the error bars. For example, at -15 °C the [INP] increases from 0.28 L^{-1} to 0.46 L^{-1} in the cold air mass after the passage of cold front B. Recalling that the air masses behind cold front B contained a lower aerosol particle concentration, this suggests that the marine particles in that air mass are more efficient INPs than in the air masses

280 with more continental influence.

Although the majority of the field studies performed to measure the [INP] have been conducted in mid-latitudes, we compare with results for the few published studies from tropical latitudes and tropical coastal locations. Rosinski et al. (1988) measured the [INP] in the condensation freezing mode for particles in the GoM during a cruise. The study reports very efficient INPs with onset

285 freezing temperatures as high as -4 °C for particles with diameters between 0.1 μm and 0.4 μm. On August 6, 1986 (the closest sampling site to Sisal in the GoM) the study shows that the [INP] at -15 °C was on the order of 10^{-2} L^{-1} for particles with sizes between 0.1 μm and 0.4 μm. The results from Rosinski et al. (1988) differ from the present results where the [INP] at -15 °C was found to vary between 10^{-1} L^{-1} and 10^0 L^{-1} for particles ranging between 0.32 μm and 10 μm.

290 This discrepancy could be attributed to the differences in the size of the particles sampled. As shown by DeMott et al. (2010) particles larger than 500 nm are the more likely potential INPs and as stated by Mason et al. (2016) super-micron particles are a large contributor to the INP population. Additionally, the chemical composition of the aerosol particles collected by Rosinski et al. (1988) indicate that the air masses in the GoM in July-August were largely influenced by mineral dust

295 particles. This is further discussed below.

3.2.1 [INP] vs. particle size

Figure 6 shows the mean [INP] concentration as a function of particle size between 0.32 μm and 10 μm at four different temperatures (-15 °C, -20 °C, -25 °C, -30 °C). The INP size distributions

were different for the temperatures considered, in contrast with the results obtained by Mason et al.
300 (2015b) at the Pacific coast of Canada. At -15 °C the peak concentration was found to be in particles
ranging between 1.0 μm and 1.8 μm. This has been reported as the typical size for airborne bacteria
(Burrows et al., 2009). Similar size distributions were obtained at -20 °C and -25 °C with a peak
concentration for particles ranging in size between 3.2 μm and 5.6 μm. Finally, at -30 °C the peak
was observed at smaller sizes (i.e., between 1.8 μm and 3.2 μm). Figure 6 also shows that most
305 of the INPs are in the supermicron size range, where submicron particles represent less than 10 %
of the total [INP] independent of temperature in agreement with the results found by Mason et al.
(2015b) and Mason et al. (2016).

3.3 Identification of the Potential INP Sources

The chemical analyzes of the sampled aerosol particles indicate that a large fraction of the particle
310 mass (for sizes between 0.18 μm to 10.0 μm) are likely of marine origin (Figure 7(A-B)). Both
techniques, i.e., XRF and HPLC found that the main elements/cations/ions are sodium and chlorine.
The low concentrations of Ti, Cu, and Zn shows the very low probability of anthropogenic influence
at the sampling site. However, although sulfate and ammonium can be emitted by natural sources,
their presence, in addition to nitrates, indicate that the influence of anthropogenic activities to the
315 aerosol population is not completely negligible. Finally, the low concentration of Al, Fe, and Si
suggest that mineral dust is not a major contributor of aerosol particle mass during the sampling
period. The long-range transport of mineral dust particles from Africa to the Yucatan Peninsula and
the GoM is very rare between January and February, compared with the more frequent transport
probability during July-August (Rosinski et al., 1988; Kishcha et al., 2014). Rosinski et al. (1988)
320 reported that the concentration of Al, Fe, and Si in July-August 1986 in the GoM were higher than
the sodium and chlorine concentrations, although the aerosol was supposed to be of marine origin.

Figure 7(C-D) show the mass size distribution of the main five elements/cations/ions determined
by the XRF and HPLC techniques. For the XRF analyzes Na, Cl, and Ca, have a single peak at
3.2 μm, whereas the S and Mg reported two peaks at 0.32 μm and 3.2 μm. Similar to the XRF
325 results, the HPLC analyzes for Na^+ and Cl^- also showed a single peak at 3.2 μm. SO_4^{2-}, NO_3^-
showed two peaks at 0.32 μm and 3.2 μm, whereas for NH_4^+ the peaks were located at 0.32 μm
and 5.6 μm. The obtained size distributions are in agreement with those of sea salt type particles
as reported elsewhere (O'dowd et al., 2004; Prather et al., 2013). Given the low resolution of these
measurements (i.e, 48 h) we were unable to quantitatively separate the chemical composition of the
330 aerosol particles during the passage of cold fronts to identify the composition of the efficient INPs
observed.

Given that mineral dust particles are unlikely the source of the measured INPs above -12 °C, and
as organics and soot are not typically efficient INPs at temperatures above -15 °C (Kanji et al., 2017),
in addition to the supermicron size of ca. 90 % of the INPs, bioparticles are the best candidates as the

335   source of INP, as bioparticles have been shown to efficiently nucleate ice at those high temperatures
(Hoose and Möhler, 2012; Murray et al., 2012; Ladino et al., 2013). To confirm the presence of
bioparticles around Sisal and to determine their potential role in the ice nucleating abilities of the
collected aerosol particles, bacteria and fungi identification was performed.

Samples for viable bacteria and fungi were collected every day at 6:00, 8:00, 10:00, and 12:00
340   local time. However, a single daily profile was performed between January 22 and 23. Bacteria
and fungi colony forming units (cfu) m^{-3} were usually above zero with the highest concentrations
found early in the morning (Figure S4). The bacteria and fungi concentrations showed a relatively
good correlation (r=0.55, p<0.0005 not shown) with average values for the whole sampling period
of 295±312 cfu m^{-3} and 438±346 cfu m^{-3}, respectively. The bacteria concentration are compa-
345   rable to the values found by Hurtado et al. (2014) in Tijuana, on the Pacific coast of Mexico (i.e,
230 cfu m^{-3} - 280 cfu m^{-3}). Bacteria and fungi concentrations were found to be lower when the
wind was coming from the north in comparison with southern-continental air masses (Figure S5), a
behavior similar to the aerosol concentration shown in section 3.2.

Figure 8 shows the time series of the [INP] together with the bacteria and fungal concentrations.
350   Panels B and C show a poor correlation between the bacteria and fungal concentrations with the
[INP] with correlation coefficients at -15 °C of 0.12 (p=0.06) and 0.36 (p=0.03), respectively. This
poor correlation can be in part due to the different timings of the MOUDI and the biosamplers which
lead to uncertainties in the analysis. Another additional factor is the fact that the reported bacteria
and fungi concentrations are only a small fraction of the total population given that the used method
355   is selective to viable microorganisms only. Note that the fraction of detected microorganisms by
culture methods are typically ca. 1 % (but can be lower) of the total population (Lighthart, 2000;
Burrows et al., 2009). From Figure 8 it is notable that although the bacteria and fungi concentrations
were very low on January 29 (i.e., under the influence of the cold front B), the [INP] at -15 °C was
comparable to the average value for the entire campaign. It is therefore intriguing if the marine
360   microorganisms brought to Sisal by the cold front B could be efficient INPs.

Table 2 summarizes the identified bacteria before the arrival of cold front A and after the passage
of cold fronts A and B. Additionally, Table 3 shows the fungi identification for the whole campaign.
To our knowledge this is the first time that airborne viable bacteria, and fungi are identified at this
coastal location. Although biological microorganism characterization has been previously conducted
365   in Mexico, those studies focused on health effects mainly (Santos-Burgoa et al., 1994; Guzman,
1998; Maldonado et al., 2009; Frías-De León et al., 2016; Ríos et al., 2016). Note that 76 % of the
detected bacteria were Gram positive with *Micrococcus*, *Staphylococcus*, and *Bacillus* as the main
identified genus (Figure S6). As shown in Table 2, before the arrival of cold front A (January 21-22),
a large variety of bacteria species were found with different typical sources, mostly terrestrial. This
370   is in contrast with the identified species found after the passage of cold fronts A and B. Especially,
after cold front B different *Vibrio* species were identified, most of which are typically of marine

origin. Recently, Hurtado et al. (2014) found that the most common genera of the bacteria in Tijuana were *Staphylococcus*, *Streptococcus*, *Pseudomonas*, and *Bacillus* in close agreement with the present results.

375 Regarding fungi, different genus were also identified as shown in Table 3 with *Cladosporium* and *Penicillium* as the most frequent ones (51 % and 11 %, respectively) as shown in Figure S6. This is in good agreement with the data reported by Després et al. (2012).

Several studies haven shown the good correlation between the concentration of fluorescent biological particles and the [INP]; however, from those studies it is highly uncertain if the good ice

380 nucleating abilities can be attributed to a single microorganism specie (Mason et al., 2015b; Twohy et al., 2016). Off-line methods as the one used here have been able to identify from rain water and cloud water specific microorganisms such as *Pseudomonas syringae*, *Micrococcus*, *Staphylococcus*, *Cladosporium*, *Penicillium*, *Aspergillus* among others, with some showing good ice nucleating ability (Amato et al., 2007, 2017; Delort et al., 2010; Failor et al., 2017; Stopelli et al., 2017; Akila et al.,

385 2018).

4   Conclusions

Aerosol particles around Sisal (on the northwest coast of the Yucatan peninsula) were found to be efficient INPs with onset freezing temperatures as high as -3 °C, similar to the onset freezing temperature of the well known efficient INP *Pseudomonas syringae* (Wex et al., 2015) and Arctic

390 sea surface microlayer organic-enriched waters (Wilson et al., 2015). The results show that the INPs concentration in Sisal are comparable (in specific cases even higher) than at other locations studied using the same INP counter type, especially under the influence of cold fronts. This is an intriguing result given that the air masses behind the cold front contained lower aerosol particles concentrations. This deserves further analysis given than the Yucatan peninsula and the Caribbean

395 region are impacted by this meteorological phenomenon during the winter and early spring months.

The chemical analyzes performed on the sampled aerosol particles did not indicate the presence of mineral dust particles in significant concentrations (the combined mass concentrations of Al, Si, and Fe correspond to 5.1 % of the total particle mass measured by the XRF), not surprisingly since African dust is mainly transported to South America during January (Prospero et al., 2014). The

400 large concentration of INPs above -15 °C, and the large size of 90 % of the INPs, indicate that the likely source of the INPs measured in Sisal are biological particles. Therefore, continental and probably maritime biological particles are believed to play an important role in ice cloud formation and precipitation development in the Yucatan peninsula. Although several bacteria and fungi were identifiied, it is unknown if any of them were responsible for the observed ice nucleating abilities of

405 the aerosol around Sisal. As stated by Islebe et al. (2015) both bacteria and fungi need to be properly documented in the peninsula and the GoM to fully understand their regional importance.

The quantitative understanding of the importance of biological particles in ice particle formation is a challenging task for the cloud physics community. As shown here, even when combining biology with chemistry, physics, and meteorology, the results obtained are not as quantitative as would be desired. Efficient INPs such as those measured in Sisal could be very important for cloud glaciation. Additionally, they can trigger ice multiplication or secondary ice formation at such high temperatures via the Hallett-Mossop mechanism (Hallett and Mossop, 1974; Field et al., 2017) and impact precipitation formation. Therefore, further studies are needed in order to improve our current limited understanding of the role that tropical microorganisms could play in ice cloud formation.

415 *Author contributions*. LAL and GBR designed the experiments. LAL, HAO, MAE, and BF carried out the INP and aerosol measurements. IR, LM, ES,EQ, LAM, and AGR analyzed the biological particles. HAO and JM performed the chemical analyzes. LAL, ZRD, CC, AKB, MS and VI performed the INP analyzes. LAL wrote the paper, with contributions from all co-authors.

Acknowledgements. The authors thank E. Garcia, G. Chavez, I. Gavilan, R. Gutierrez, J. Munoz, L. Landeros,
420 W. Gutierrez, M. Garcia, M. Robles, A. Rodriguez, J.C. Pineda, L. Gonzalez, A. Prieto, T. Castro, M.I. Saavedra, and A. Cruz for their invaluable help. We also thank David S. Valdes from CINVESTAV Merida for sharing the meteorological data. This study was financially supported by the Direccion General de Asuntos del Personal Academico (DGAPA) and by the Consejo Nacional de Ciencia y Tecnologia (Conacyt) through grants PAPIIT IA108417 and IN102818 and I000/781/2106.

References

425

Akila, M., Priyamvada, H., Ravikrishna, R., and Gunthe, S. S.: Characterization of bacterial diversity and ice-
nucleating ability during different monsoon seasons over a southern tropical Indian region, Atmos. Environ.,
191, 387–394, doi:10.1016/j.atmosenv.2018.08.026, 2018.

Amato, P., Parazols, M., Sancelme, M., Laj, P., Mailhot, G., and Delort, A.-M.: Microorganisms isolated
430   from the water phase of tropospheric clouds at the Puy de Dôme: major groups and growth abilities at low
temperatures, FEMS Microbiol. Ecol., 59, 242–254, doi:10.1111/j.1574-6941.2006.00199.x, 2007.

Amato, P., Joly, M., Besaury, L., Oudart, A., Taib, N., Moné, A. I., Deguillaume, L., Delort, A.-M., and
Debroas, D.: Active microorganisms thrive among extremely diverse communities in cloud water, PloS one,
12, e0182 869, doi:10.1371/journal.pone.0182869, 2017.

435   Andreae, M. and Rosenfeld, D.: Aerosol–cloud–precipitation interactions. Part 1. The nature and sources of
cloud-active aerosols, Earth Sci. Rev., 89, 13–41, doi:10.1016/j.earscirev.2008.03.001, 2008.

Atkinson, J. D., Murray, B. J., Woodhouse, M. T., Whale, T. F., Baustian, K. J., Carslaw, K. S., Dobbie, S.,
OSullivan, D., and Malkin, T. L.: The importance of feldspar for ice nucleation by mineral dust in mixed-
phase clouds, Nature, 498, 355, doi:10.1038/nature12278, 2013.

440   Bateman, A. P., Belassein, H., and Martin, S. T.: Impactor apparatus for the study of particle rebound: Rela-
tive humidity and capillary forces, Aerosol Sci. Techonol., 48, 42–52, doi:10.1080/02786826.2013.853866,
2014.

Boose, Y., Sierau, B., García, M. I., Rodríguez, S., Alastuey, A., Linke, C., Schnaiter, M., Kupiszewski, P.,
Kanji, Z. A., and Lohmann, U.: Ice nucleating particles in the Saharan Air Layer, Atmos. Chem. Phys., 16,
445   9067–9087, doi:10.5194/acp-16-9067-2016, 2016.

Burrows, S. M., Elbert, W., Lawrence, M., and Pöschl, U.: Bacteria in the global atmosphere–Part 1: Review
and synthesis of literature data for different ecosystems, Atmos. Chem. Phys., 9, 9263–9280, doi:10.5194/
acp-9-9263-2009, 2009.

Burrows, S. M., Hoose, C., Pöschl, U., and Lawrence, M.: Ice nuclei in marine air: biogenic particles or dust?,
450   Atmos. Chem. Phys., 13, 245–267, doi:10.5194/acp-13-245-2013, 2013.

Chen, S.-C., Tsai, C.-J., Chen, H.-D., Huang, C.-Y., and Roam, G.-D.: The influence of relative humidity
on nanoparticle concentration and particle mass distribution measurements by the MOUDI, Aerosol Sci.
Technol., 45, 596–603, doi:10.1080/02786826.2010.551557, 2011.

Chow, J. C. and Watson, J. G.: Ion chromatography in elemental analysis of airborne particles, Elemental
455   analysis of airborne particles, 1, 97–137, 1999.

DeLeon-Rodriguez, N., Lathem, T. L., Rodriguez-R, L. M., Barazesh, J. M., Anderson, B. E., Beyersdorf, A. J.,
Ziemba, L. D., Bergin, M., Nenes, A., and Konstantinidis, K. T.: Microbiome of the upper troposphere:
species composition and prevalence, effects of tropical storms, and atmospheric implications, P. Natl. Acad.
Sci., 110, 2575–2580, doi:10.1073/pnas.1212089110, 2013.

460   Delort, A.-M., Vaïtilingom, M., Amato, P., Sancelme, M., Parazols, M., Mailhot, G., Laj, P., and Deguillaume,
L.: A short overview of the microbial population in clouds: Potential roles in atmospheric chemistry and
nucleation processes, Atmos. Res., 98, 249–260, doi:10.1016/j.atmosres.2010.07.004, 2010.

DeMott, P. J., Prenni, A. J., Liu, X., Kreidenweis, S. M., Petters, M. D., Twohy, C. H., Richardson, M.,
Eidhammer, T., and Rogers, D.: Predicting global atmospheric ice nuclei distributions and their impacts on

465   climate, P. Natl. Acad. Sci., 107, 11 217–11 222, doi:10.1073/pnas.0910818107, 2010.

DeMott, P. J., Hill, T. C., McCluskey, C. S., Prather, K. A., Collins, D. B., Sullivan, R. C., Ruppel, M. J., Mason, R. H., Irish, V. E., Lee, T., et al.: Sea spray aerosol as a unique source of ice nucleating particles, P. Natl. Acad. Sci., 113, 5797–5803, doi:10.1073/pnas.1514034112, 2016.

Després, V., Huffman, J. A., Burrows, S. M., Hoose, C., Safatov, A., Buryak, G., Fröhlich-Nowoisky, J., Elbert,
470   W., Andreae, M., Pöschl, U., et al.: Primary biological aerosol particles in the atmosphere: a review, Tellus B, 64, 15 598, doi:10.3402/tellusb.v64i0.15598, 2012.

Espinosa, A., Miranda, J., and Pineda, J.: Uncertainty evaluation in correlated quantities: application to elemental analysis of atmospheric aerosols, Rev. Mex. Fis., E56, 134–140, 2010.

Espinosa, A., Reyes-Herrera, J., Miranda, J., Mercado, F., Veytia, M., Cuautle, M., and Cruz, J.: Development
475   of an X-ray fluorescence spectrometer for environmental science applications, Instr. Sci. Technol., 40, 603–617, doi:10.1080/10739149.2012.693560, 2012.

Failor, K., Schmale Iii, D., Vinatzer, B., and Monteil, C. L.: Ice nucleation active bacteria in precipitation are genetically diverse and nucleate ice by employing different mechanisms, ISME J., 11, 2740, doi:10.1038/ismej.2017.124, 2017.

480   Field, P. R., Lawson, R. P., Brown, P. R., Lloyd, G., Westbrook, C., Moisseev, D., Miltenberger, A., Nenes, A., Blyth, A., Choularton, T., et al.: Secondary Ice Production: Current State of the Science and Recommendations for the Future, Meteorol. Monogr., 58, 7.1–7.20, doi:10.1175/AMSMONOGRAPHS-D-16-0014.1, 2017.

Fitzgerald, J. W.: Marine aerosols: A review, Atmos. Environ., 25, 533–545, doi:10.1016/0960-1686(91)
485   90050-H, 1991.

Frías-De León, M. G., Duarte-Escalante, E., del Carmen Calderón-Ezquerro, M., del Carmen Jiménez-Martínez, M., Acosta-Altamirano, G., Moreno-Eutimio, M. A., Zúñiga, G., García-González, R., Ramírez-Pérez, M., and del Rocío Reyes-Montes, M.: Diversity and characterization of airborne bacteria at two health institutions, Aerobiologia, 32, 187–198, doi:10.1007/s10453-015-9389-z, 2016.

490   Fröhlich-Nowoisky, J., Hill, T. C., Pummer, B. G., Yordanova, P., Franc, G. D., and Pöschl, U.: Ice nucleation activity in the widespread soil fungus Mortierella alpina, Biogeosciences, 12, 1057, doi:10.5194/bg-12-1057-2015, 2015.

Fröhlich-Nowoisky, J., Kampf, C. J., Weber, B., Huffman, J. A., Pöhlker, C., Andreae, M. O., Lang-Yona, N., Burrows, S. M., Gunthe, S. S., Elbert, W., et al.: Bioaerosols in the Earth system: Climate, health, and
495   ecosystem interactions, Atmos. Res., 182, 346–376, doi:10.1016/j.atmosres.2016.07.018, 2016.

Galtier, N., Gouy, M., and Gautier, C.: SEAVIEW and PHYLO_WIN: two graphic tools for sequence alignment and molecular phylogeny, Bioinformatics, 12, 543–548, doi:10.1093/bioinformatics/12.6.543, 1996.

Guzmán, G.: New species of fungi from the Yucatan Peninsula, Mycotaxon, 1982.

Guzman, G. N.: Inventorying the fungi of Mexico, Biodivers. Conserv., 7, 369–384, 1998.

500   Hallett, J. and Mossop, S.: Production of secondary ice particles during the riming process, Nature, 249, 26, 1974.

Hill, T. C., DeMott, P., Conen, F., and Möhler, O.: Impacts of Bioaerosols on Atmospheric Ice Nucleation Processes, Microbiol. Aerosol., p. 197, 2017.

Hoose, C. and Möhler, O.: Heterogeneous ice nucleation on atmospheric aerosols: a review of results from

505   laboratory experiments, Atmos. Chem. Phys., 12, 98179854, doi:10.5194/acp-12-9817-2012, 2012.

Hoose, C., Kristjánsson, J., and Burrows, S.: How important is biological ice nucleation in clouds on a global scale?, Environ. Res. Lett., 5, 024 009, doi:10.1088/1748-9326/5/2/024009, 2010.

Hurtado, L., Rodríguez, G., López, J., Castillo, J., Molina, L., Zavala, M., and Quintana, P. J.: Characterization of atmospheric bioaerosols at 9 sites in Tijuana, Mexico, Atmos. Environ., 96, 430–436, doi:10.1016/j.

510   atmosenv.2014.07.018, 2014.

IAEA: Manual for QXAS, International Atomic Energy Agency, p. Vienna, 1997.

Irish, V. E., Elizondo, P., Chen, J., Chou, C., Charette, J., Lizotte, M., Ladino, L. A., Wilson, T. W., Gosselin, M., Murray, B. J., et al.: Ice-nucleating particles in Canadian Arctic sea-surface microlayer and bulk seawater, Atmos. Chem. Phys., 17, 10 583–10 595, doi:10.5194/acp-17-10583-2017, 2017.

515 Islebe, G. A., Calmé, S., León-Cortés, J. L., and Schmook, B.: Biodiversity and conservation of the Yucatán Peninsula, Springer, 2015.

Kanji, Z. A., Ladino, L. A., Wex, H., Boose, Y., Burkert-Kohn, M., Cziczo, D. J., and Krämer, M.: Overview of ice nucleating particles, Meteorol. Monogr., 58, 1.1–1.33, doi:10.1175/AMSMONOGRAPHS-D-16-0006.1, 2017.

520 Kishcha, P., da Silva, A., Starobinets, B., Long, C., Kalashnikova, O., and Alpert, P.: Meridional distribution of aerosol optical thickness over the tropical Atlantic Ocean, Atmos. Chem. Phys. Discuss., 14, 23 309–23 339, doi:10.5194/acpd-14-23309-2014, 2014.

Knopf, D., Alpert, P., Wang, B., and Aller, J.: Stimulation of ice nucleation by marine diatoms, Nat. Geosci., 4, 88, doi:10.1038/NGEO1037, 2011.

525 Knutson, T. R., McBride, J. L., Chan, J., Emanuel, K., Holland, G., Landsea, C., Held, I., Kossin, J. P., Srivastava, A., and Sugi, M.: Tropical cyclones and climate change, Nat. Geosci., 3, 157, doi:10.1038/ngeo779, 2010.

Ladino, L., Stetzer, O., and Lohmann, U.: Contact freezing: a review of experimental studies, Atmos. Chem. Phys., 13, 9745–9769, doi:10.5194/acp-13-9745-2013, 2013.

530 Ladino, L., Yakobi-Hancock, J., Kilthau, W., Mason, R., Si, M., Li, J., Miller, L., Schiller, C., Huffman, J., Aller, J., et al.: Addressing the ice nucleating abilities of marine aerosol: A combination of deposition mode laboratory and field measurements, Atmos. Environ., 132, 1–10, doi:10.1016/j.atmosenv.2016.02.028, 2016.

Landsea, C.: Counting Atlantic tropical cyclones back to 1900, Eos, 88, 197–202, doi:10.1029/2007EO180001, 2007.

535 Lane, D.: 16S/23S rRNA sequencing. In Nucleic acid techniques in bacterial systematics.(Eds E Stackebrandt, M Goodfellow) pp. 115–175, 1991.

Lighthart, B.: Mini-review of the concentration variations found inthe alfresco atmospheric bacterial populations, Aerobiologia, 16, 7–16, 2000.

Lohmann, U. and Feichter, J.: Global indirect aerosol effects: a review, Atmos. Chem. Phys., 5, 715–737,

540   doi:10.5194/acp-5-715-2005, 2005.

Maldonado, L. A., Stach, J. E., Ward, A. C., Bull, A. T., and Goodfellow, M.: Characterisation of micromonosporae from aquatic environments using molecular taxonomic methods, Anton. Leeuw., 94, 289–298, doi:10.1007/s10482-008-9244-0, 2008.

Maldonado, L. A., Fragoso-Yáñez, D., Pérez-García, A., Rosellón-Druker, J., and Quintana, E. T.: Acti-

545   nobacterial diversity from marine sediments collected in Mexico, Anton. Leeuw., 95, 111–120, doi:
        10.1007/s10482-008-9294-3, 2009.

        Mason, R., Chou, C., McCluskey, C., Levin, E., Schiller, C., Hill, T., Huffman, J., DeMott, P., and Bertram,
        A.: The micro-orifice uniform deposit impactor–droplet freezing technique (MOUDI-DFT) for measuring
        concentrations of ice nucleating particles as a function of size: improvements and initial validation, Atmos.
550   Meas. Tech., 8, 2449–2462, doi:10.5194/amt-8-2449-2015, 2015a.

        Mason, R., Si, M., Li, J., Chou, C., Dickie, R., Toom-Sauntry, D., Pöhlker, C., Yakobi-Hancock, J., Ladino, L.,
        Jones, K., et al.: Ice nucleating particles at a coastal marine boundary layer site: correlations with aerosol type
        and meteorological conditions, Atmos. Chem. Phys., 15, 12 547–12 566, doi:10.5194/acp-15-12547-2015,
        2015b.

555   Mason, R., Si, M., Chou, C., Irish, V., Dickie, R., Elizondo, P., Wong, R., Brintnell, M., Elsasser, M., Lassar,
        W., et al.: Size-resolved measurements of ice-nucleating particles at six locations in North America and one
        in Europe, Atmos. Chem. Phys., 16, 1637–1651, doi:10.5194/acp-16-1637-2016, 2016.

        Mayol, E., Arrieta, J. M., Jiménez, M. A., Martínez-Asensio, A., Garcias-Bonet, N., Dachs, J., González-Gaya,
        B., Royer, S.-J., Benítez-Barrios, V. M., Fraile-Nuez, E., et al.: Long-range transport of airborne microbes
560   over the global tropical and subtropical ocean, Nat. Commun., 8, 201, doi:10.1038/s41467-017-00110-9,
        2017.

        McCluskey, C. S., Hill, T. C., Malfatti, F., Sultana, C. M., Lee, C., Santander, M. V., Beall, C. M., Moore,
        K. A., Cornwell, G. C., Collins, D. B., et al.: A Dynamic Link between Ice Nucleating Particles Released in
        Nascent Sea Spray Aerosol and Oceanic Biological Activity during Two Mesocosm Experiments, J. Atmos.
565   Sci., 74, 151–166, doi:10.1175/JAS-D-16-0087.1, 2017.

        Michaud, J., Luke, T., Drishti, K., Josh, E., Alexander, R., Zhenjiang, Z., Christopher, L., Kevin, P., Charlotte,
        B., Francesca, M., Farooq, A., Rob, K., Michael, B., Christopher, D., and Kimberly, P.: Taxon-specific
        aerosolization of bacteria and viruses in an experimental ocean-atmosphere mesocosm, Nat. Commun., 18,
        1–10, doi:10.1038/s41467-018-04409-z, 2018.

570   Morales, J. L., Cantillo-Ciau, Z. O., Sánchez-Molina, I., and Mena-Rejón, G. J.: Screening of antibacterial and
        antifungal activities of six marine macroalgae from coasts of Yucatan peninsula, Pharm. Biol., 44, 632–635,
        doi:10.1080/13880200600897569, 2006.

        Mülmenstädt, J., Sourdeval, O., Delanoë, J., and Quaas, J.: Frequency of occurrence of rain from liquid-,
        mixed-, and ice-phase clouds derived from A-Train satellite retrievals, Geophys. Res. Lett., 42, 6502–6509,
575   doi:10.1002/2015GL064604, 2015.

        Murray, B., O'sullivan, D., Atkinson, J., and Webb, M.: Ice nucleation by particles immersed in supercooled
        cloud droplets, Chem. Soc. Rev., 41, 6519–6554, doi:10.1039/C2CS35200A, 2012.

        Nenes, A., Murray, B., and Bougiatioti, A.: Mineral dust and its microphysical interactions with clouds, in:
        Mineral Dust, pp. 287–325, Springer, 2014.

580   O'dowd, C. D., Facchini, M. C., Cavalli, F., Ceburnis, D., Mircea, M., Decesari, S., Fuzzi, S., Yoon, Y. J., and
        Putaud, J.-P.: Biogenically driven organic contribution to marine aerosol, Nature, 431, 676, doi:10.1038/
        Nature02959, 2004.

        Patterson, E., Kiang, C., Delany, A., Wartburg, A., Leslie, A., and Huebert, B.: Global measurements of
        aerosols in remote continental and marine regions: Concentrations, size distributions, and optical properties,

585   J. Geophys. Res., 85, 7361–7376, doi:10.1029/JC085iC12p07361, 1980.

Prather, K. A., Bertram, T. H., Grassian, V. H., Deane, G. B., Stokes, M. D., DeMott, P. J., Aluwihare, L. I.,
        Palenik, B. P., Azam, F., Seinfeld, J. H., et al.: Bringing the ocean into the laboratory to probe the chemical
        complexity of sea spray aerosol, P. Natl. Acad. Sci., 110, 7550–7555, doi:10.1073/pnas.1300262110, 2013.

Price, H., Baustian, K., McQuaid, J., Blyth, A., Bower, K., Choularton, T., Cotton, R., Cui, Z., Field, P.,
590   Gallagher, M., et al.: Atmospheric Ice-Nucleating Particles in the Dusty Tropical Atlantic, J. Geophys. Res,
        123, 2175–2193, doi:10.1002/2017JD027560, 2018.

Prospero, J. M., Collard, F.-X., Molinié, J., and Jeannot, A.: Characterizing the annual cycle of African dust
        transport to the Caribbean Basin and South America and its impact on the environment and air quality, Global
        Biogeochem. Cy., 28, 757–773, doi:10.1002/2013GB004802, 2014.

595   Ramanathan, V., Cess, R., Harrison, E., Minnis, P., Barkstrom, B., Ahmad, E., and Hartmann, D.: Cloud-
        radiative forcing and climate: Results from the Earth Radiation Budget Experiment, Science, 243, 57–63,
        doi:10.1126/science.243.4887.57, 1989.

Ríos, B., Torres-Jardón, R., Ramírez-Arriaga, E., Martínez-Bernal, A., and Rosas, I.: Diurnal variations of
        airborne pollen concentration and the effect of ambient temperature in three sites of Mexico City, Int. J.
600   Biometeorol., 60, 771–787, doi:10.1007/s00484-015-1061-3, 2016.

Rosinski, J., Haagenson, P., Nagamoto, C., and Parungo, F.: Nature of ice-forming nuclei in marine air masses,
        J. Aerosol Sci., 18, 291–309, doi:10.1016/0021-8502(87)90024-3, 1987.

Rosinski, J., Haagenson, P., Nagamoto, C., Quintana, B., Parungo, F., and Hoyt, S.: Ice-forming nuclei in air
        masses over the Gulf of Mexico, J. Aerosol Sci., 19, 539–551, doi:10.1016/0021-8502(88)90206-6, 1988.

605   Santos-Burgoa, C., Rosas, I., and Yela, A.: Occurrence of airborne enteric bacteria in Mexico City, Aerobi-
        ología, 10, 39–45, 1994.

Schnell, R.: Ice nuclei produced by laboratory cultured marine phytoplankton, Geophys. Res. Lett., 2, 500–502,
        doi:10.1029/GL002i011p00500, 1975.

Schnell, R.: Ice nuclei in seawater, fog water and marine air off the coast of Nova Scotia: Summer 1975, J.
610   Atmos. Sci., 34, 1299–1305, doi:10.1175/1520-0469(1977)034⟨1299:INISFW⟩2.0.CO;2, 1977.

Schnell, R.: Airborne ice nucleus measurements around the Hawaiian Islands, J. Geophys. Res, 87, 8886–8890,
        doi:10.1029/JC087iC11p08886, 1982.

Schnell, R. and Vali, G.: Freezing nuclei in marine waters, Tellus, 27, 321–323, doi:10.1111/j.2153-3490.1975.
        tb01682.x, 1975.

615   SEDESOL: Secretaria   de   desarrollo   social: Catalogo   de   localidades,
        http://www.microrregiones.gob.mx/catloc/contenido.aspx?refnac=310380004, 2015.

Seinfeld, J. H., Bretherton, C., Carslaw, K. S., Coe, H., DeMott, P. J., Dunlea, E. J., Feingold, G., Ghan,
        S., Guenther, A. B., Kahn, R., et al.: Improving our fundamental understanding of the role of aerosol- cloud
        interactions in the climate system, P. Natl. Acad. Sci., 113, 5781–5790, doi:10.1073/pnas.1514043113, 2016.

620   Sesartic, A., Lohmann, U., and Storelvmo, T.: Bacteria in the ECHAM5-HAM global climate model, Atmos.
        Chem. Phys., 12, 8645–8661, doi:10.5194/acp-12-8645-2012, 2012.

Stevens, B. and Feingold, G.: Untangling aerosol effects on clouds and precipitation in a buffered system,
        Nature, 461, 607, doi:10.1038/nature08281, 2009.

Stocker, T. F., Qin, D., Plattner, G., Tignor, M., Allen, S., Boschung, J., Nauels, A., Xia, Y., Bex, V., and

625   Midgley, P.: Climate change 2013: the physical science basis. Intergovernmental panel on climate change, working group I contribution to the IPCC fifth assessment report (AR5), New York, 2013.

Stopelli, E., Conen, F., Guilbaud, C., Zopfi, J., Alewell, C., and Morris, C. E.: Ice nucleators, bacterial cells and Pseudomonas syringae in precipitation at Jungfraujoch, Biogeosciences, 14, 1189–1196, doi:10.5194/bg-14-1189-2017, 2017.

630   Twohy, C. H., McMeeking, G. R., DeMott, P. J., McCluskey, C. S., Hill, T. C., Burrows, S. M., Kulkarni, G. R., Tanarhte, M., Kafle, D. N., and Toohey, D. W.: Abundance of fluorescent biological aerosol particles at temperatures conducive to the formation of mixed-phase and cirrus clouds, Atmos. Chem. Phys., 16, 8205–8225, doi:10.5194/acp-16-8205-2016, 2016.

Vali, G., DeMott, P., Möhler, O., and Whale, T.: A proposal for ice nucleation terminology, Atmos. Chem.

635   Phys., 15, 10 263–10 270, doi:10.5194/acp-15-10263-2015, 2015.

Vergara-Temprado, J., Murray, B. J., Wilson, T. W., O'Sullivan, D., Pringle, K. J., Ardon-Dryer, K., Bertram, A. K., Burrows, S. M., Ceburnis, D., DeMott, P. J., et al.: Contribution of feldspar and marine organic aerosols to global ice nucleating particle concentrations, Atmos. Chem. Phys., 17, 3637, doi: 10.5194/acp-17-3637-2017, 2017.

640   Videla, H. A., Guiamet, P. S., and de Saravia, S. G.: Biodeterioration of Mayan archaeological sites in the Yucatan Peninsula, Mexico, Int. Biodeter. Biodegr., 46, 335–341, doi:10.1016/S0964-8305(00)00106-2, 2000.

Welti, A., Müller, K., Fleming, Z. L., and Stratmann, F.: Concentration and variability of ice nuclei in the subtropic, maritime boundary layer, Atmos. Chem. Phys., 18, 5307–5320, doi:10.5194/acp-18-5307-2018, 2018.

645   Wex, H., Augustin-Bauditz, S., Boose, Y., Budke, C., Curtius, J., Diehl, K., Dreyer, A., Frank, F., Hartmann, S., Hiranuma, N., et al.: Intercomparing different devices for the investigation of ice nucleating particles using Snomax® as test substance, Atmos. Chem. Phys., 15, 1463–1485, doi:10.5194/acp-15-1463-2015, 2015.

Whigham, D. F., Olmsted, I., Cano, E. C., and Harmon, M. E.: The impact of Hurricane Gilbert on trees, litterfall, and woody debris in a dry tropical forest in the northeastern Yucatan Peninsula, Biotropica, pp.

650   434–441, doi:10.2307/2388263, 1991.

Wilson, T. W., Ladino, L. A., Alpert, P. A., Breckels, M. N., Brooks, I. M., Burrows, S. M., Carslaw, K. S., Huffman, J. A., Judd, C., Kilthau, W. P., et al.: A marine biogenic source of atmospheric ice-nucleating particles, Nature, 525, 234, doi:10.1038/nature14986, 2015.

Winkler, P.: Relative humidity and the adhesion of atmospheric particles to the plates of impactors, J. Aerosol

655   Sci., 5, 235–240, doi:10.1016/0021-8502(74)90058-5, 1974.

Yakobi-Hancock, J. D., Ladino, L. A., and Abbatt, J. P.: Review of Recent Developments and Shortcomings in the Characterization of Potential Atmospheric Ice Nuclei: Focus on the Tropics, Revista de Ciencias, 17, 15–34, doi:10.25100/rc.v17i3.476, 2014.

Yankofsky, S., Levin, Z., Bertold, T., and Sandlerman, N.: Some basic characteristics of bacterial freezing nu-

660   clei, J. Appl. Meteorol., 20, 1013–1019, doi:10.1175/1520-0450(1981)020⟨1013:SBCOBF⟩2.0.CO;2, 1981.

Yun, Y. and Penner, J. E.: An evaluation of the potential radiative forcing and climatic impact of marine organic aerosols as heterogeneous ice nuclei, Geophys. Res. Lett., 40, 4121–4126, doi:10.1002/grl.50794, 2013.
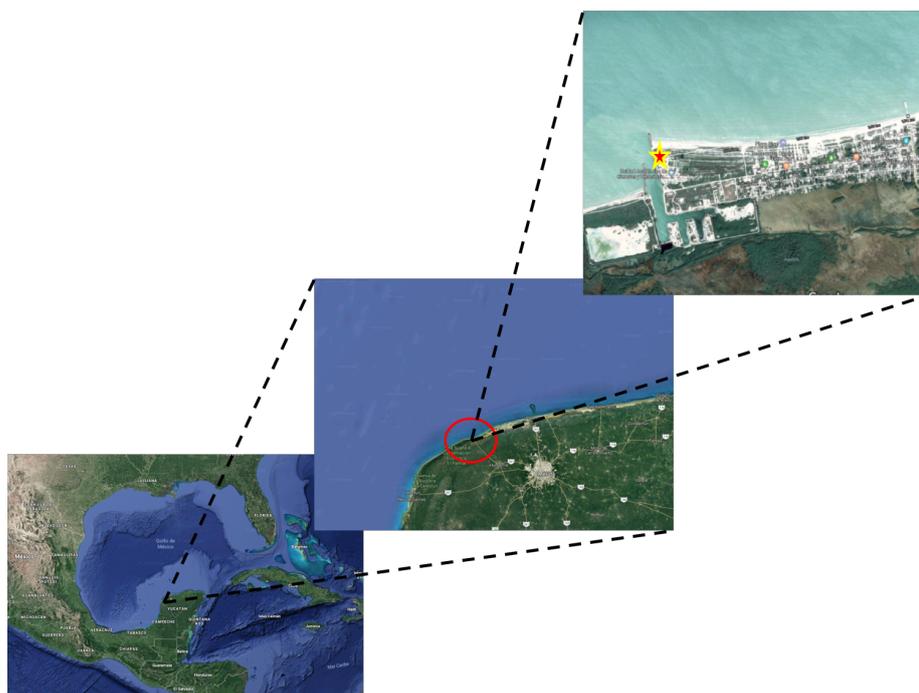
Fig. 1. Map showing the sampling location. The red star shows the location of the Engineering Institute building where the sampling took place (GoogleMaps).

Table 1. List of the measured variables and the corresponding instrumentation.

Measured Variable	Instrument
INP concentration	MOUDI-DFT (Mason et al., 2015a)
Aerosol concentration	Condensation particle counter (CPC, TSI 3010)
Coarse aerosol size distribution	LasAir Optical particle counter (MSP)
Chemical composition	X-Ray fluorescence and High-performance liquid chromatography
Bacterial and fungal concentration	Biostage impactor (SKC)
Meteorology	Weather station (Davis)
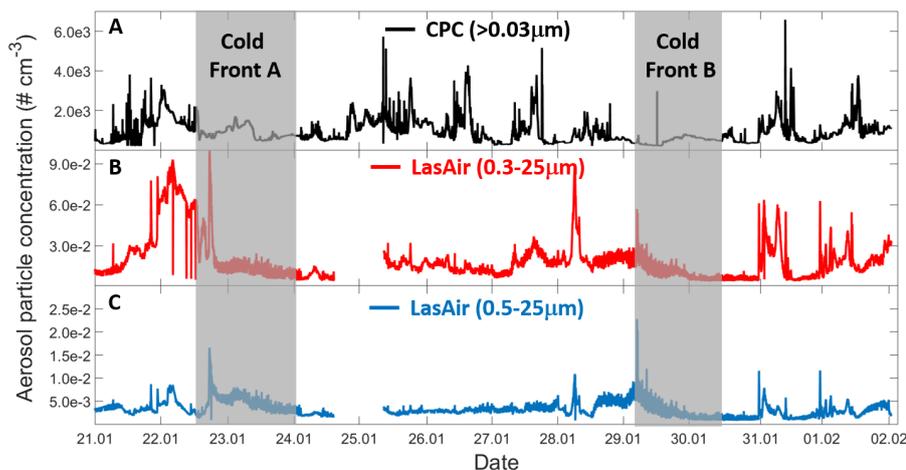
Fig. 2. Aerosol particle concentration time series for the whole campaign. A) measured by the CPC, B) measured by the LasAir full size range (0.3 μm to 25 μm), and C) measured by the LasAir for particles >500 nm (0.5 μm to 25 μm). Grey areas denote the periods affected by the entrance of a cold front (A and B). Each X-axis tick corresponds to midnight local time.
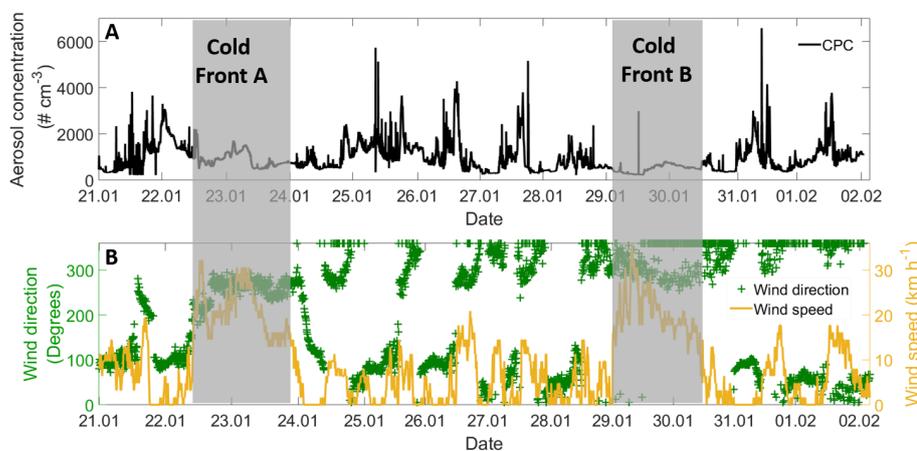
Fig. 3. A) Time series of the total aerosol particle concentration measured by the CPC, and B) Time series of the wind speed (yellow) and wind direction (green). Each X-axis tick corresponds to midnight local time.
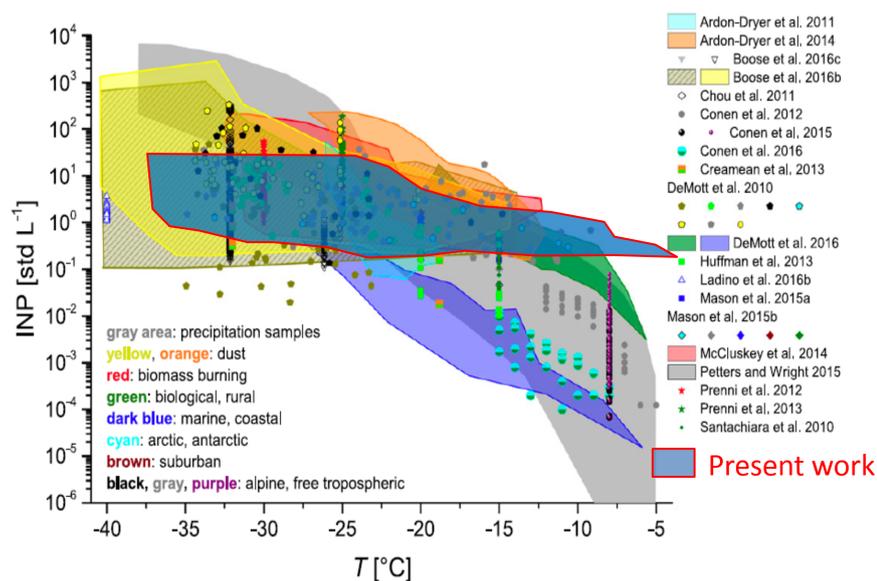
Fig. 4. Summary of INP concentrations taken from studies of field measurements conducted globally (adapted from Kanji et al. (2017)).
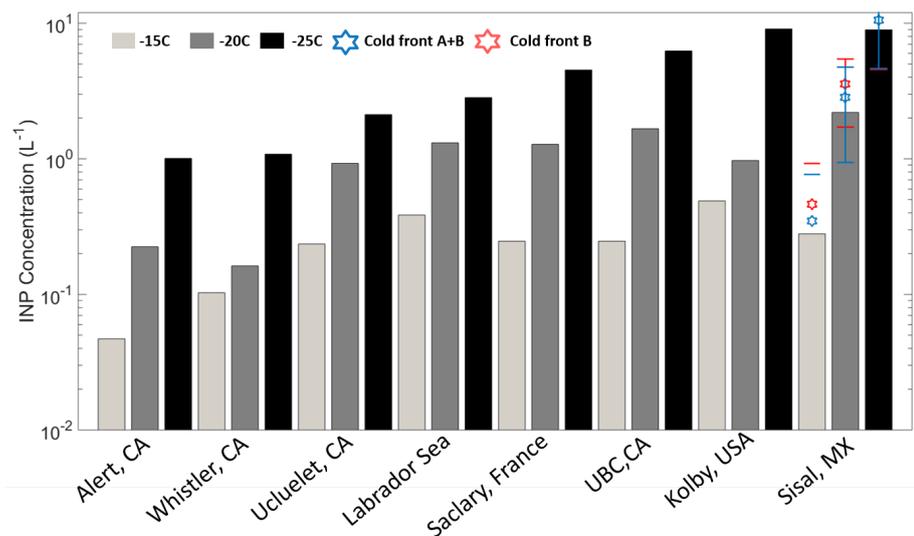
Fig. 5. Mean INP number concentrations at droplet freezing temperatures of -15 °C (light gray), -20 °C (dark gray), and -25 °C (black). The blue and red stars represent the mean INP concentration during the cold fronts A+B and cold front B, respectively (adapted from Mason et al. (2016)).
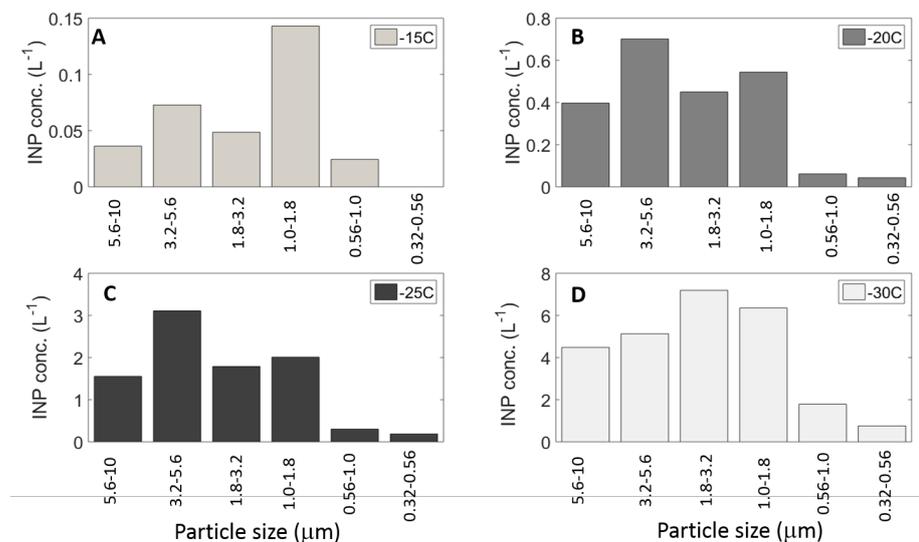
Fig. 6. Mean INP concentration as a function of aerosol particle size at A) -15 °C, B) -20 °C, C) -25 °C, and D) -30 °C.
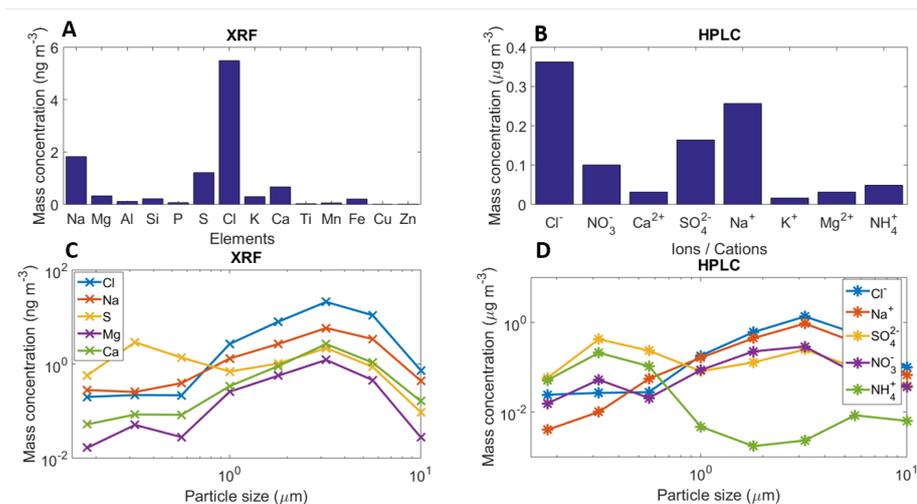
Fig. 7. A) Mean mass concentration of 14 detected elements for the collected aerosol particles using XRF, B) Mean mass concentration of 8 detected ions/cations for the collected aerosol particles using HPLC, C) and D) Mean mass size distribution of the main five detected elements/cations/ions with the XRF and HPLC, respectively.
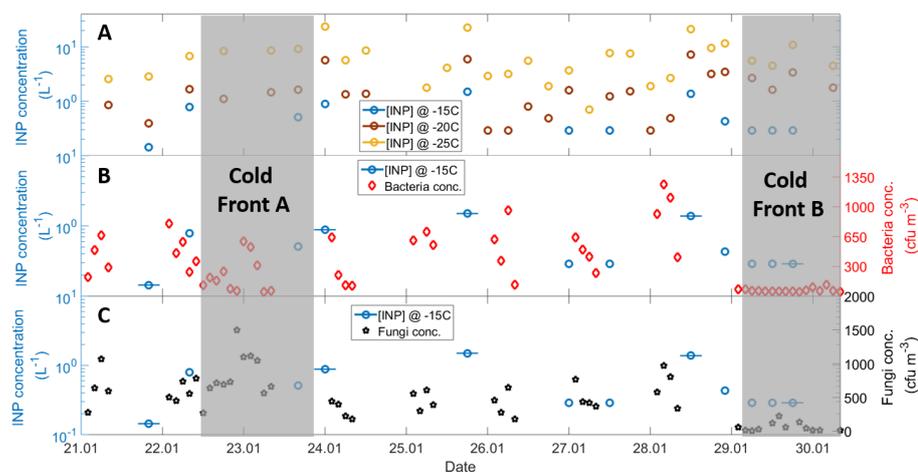
Fig. 8. A) Time series of the [INP] at -15 °C (blue), -20 °C (brown), and -25 °C (yellow), B) Time series of the [INP] at -15 °C (blue) together with bacteria concentration (red), and C) Time series of the [INP] at -15 °C (blue) together with fungal concentration (black). Each X-axis tick corresponds to 06:00 local time. The horizontal error bars indicate the time span the MOUDI-DFT measurements i.e., 6 h. Grey areas denote the periods affected by the entrance of a cold front (A and B).

Table 2. Bacterial isolation for top) Jan 21-22, middle) Cold front A, bottom) Cold front B. ^{a}, Isolated on TSA media; ^{b}, Isolated on GYM media.

Phylum	Genus/species	Source
Actinobacteria	^{a}*Kocuria palustris*	Soil, rhizoplane
	^{a}*Micrococcus* spp	Water, soil, dust, and skin
	^{a}*Rhodococcus corynebacteroides*	Soil, water and eukaryotic cells
Firmicutes	^{a}*Staphylococcus kloosii*	Human and animal skin
	^{a}*Staphylococcus lugdunensis*	Human and animal skin
	^{a}*Staphylococcus nepalensis*	Mucocutaneous zones of humans and animals
	^{a}*Staphylococcus arlettae*	Animal skin, mucosal zones, polluted water
	^{a}*Staphylococcus epidermidis*	Human skin, mucosal microbiota
	^{a}*Bacillus aryabhattai*	Upper atmosphere, rhizosphere
	^{a}*Bacillus gibsonii*	Alkaline soil
	^{a}*Bacillus aeris*	Soil
	^{a}*Staphylococcus lentus*	Soil
Alphaproteobacteria	^{a}*Sphingomonas mucosissima*	Water and soil
Actinobacteria	^{a}*Micrococcus* spp	Water, soil, dust, and skin
Firmicutes	^{a}*Bacillus oceanisediminis*	Marine sediments
Gammaproteobacteria	^{a}*Proteus mirabilis*	Water and soil
	^{a}*Pseudomonas stutzeri*	Soil
Actinobacteria	^{a,b}*Micrococcus* spp	Water, soil, dust, and skin
	^{a}*Micrococcus lentus*	Soil, dust, water and air
	^{b}*Micrococcus yunnanensis*	Roots of Polyspora axillaris
	^{b}*Streptomyces* spp	Cosmopolitan
Firmicutes	^{a}*Bacillus* spp	Cosmopolitan
	^{a}*Bacillus niacini*	Soil
	^{a}*Bacillus subtilis*	Soil, gut commensal in ruminants and humans
	^{a}*Planomicrobium koreense*	Fermented seafood
	^{a}*Staphylococcus* spp	Human and animal skin, mucous zones, soils
	^{b}*Solibacillus isronensis*	Air
	^{a}*Staphylococcus equorum*	Human and animal skin
Gammaproteobacteria	^{a}*Pseudomonas reactants*	Soil
	^{a}*Vibrio alginolyticus*	Marine
	^{a}*Vibrio natriegens*	Marine
	^{a}*Vibrio neocaledonicus*	Marine
	^{a}*Vibrio parahaemolyticus*	Marine
	^{a}*Zobellella* sp.	Marine and estuarine environments

Table 3. Fungal identification on EMA media for the whole sampling period

Phylum	Genus	Source
Dothideomycetes	*Alternaria*	
	Cladoporium	
	Drechslera	Dead plants, soil, foods, air, indoor
Euascomycetes	*Curvularia*	enviroments, decaying organic matter,
Eurotiomycetes	*Aspergillus*	bioaerosols in, on animal systems and
	Penicillium	in freshwater and marine habitats.
Leotiomycetes	*Monilia*	
Sordariomycetes	*Fusarium*	
Zygomycetes	*Rhizopus*	